Developmental Cell *17*

Supplemental Data

Coordinated Actions of Actin and BAR Proteins

Upstream of Dynamin at Endocytic Clathrin Coated Pits

Shawn Ferguson, Andrea Raimondi, Summer Paradise, Hongying Shen, Kumi Mesaki, Agnes Ferguson, Olivier Destaing, Genevieve Ko, Junko Takasaki, Ottavio Cremona, Eileen O' Toole, and Pietro De Camilli

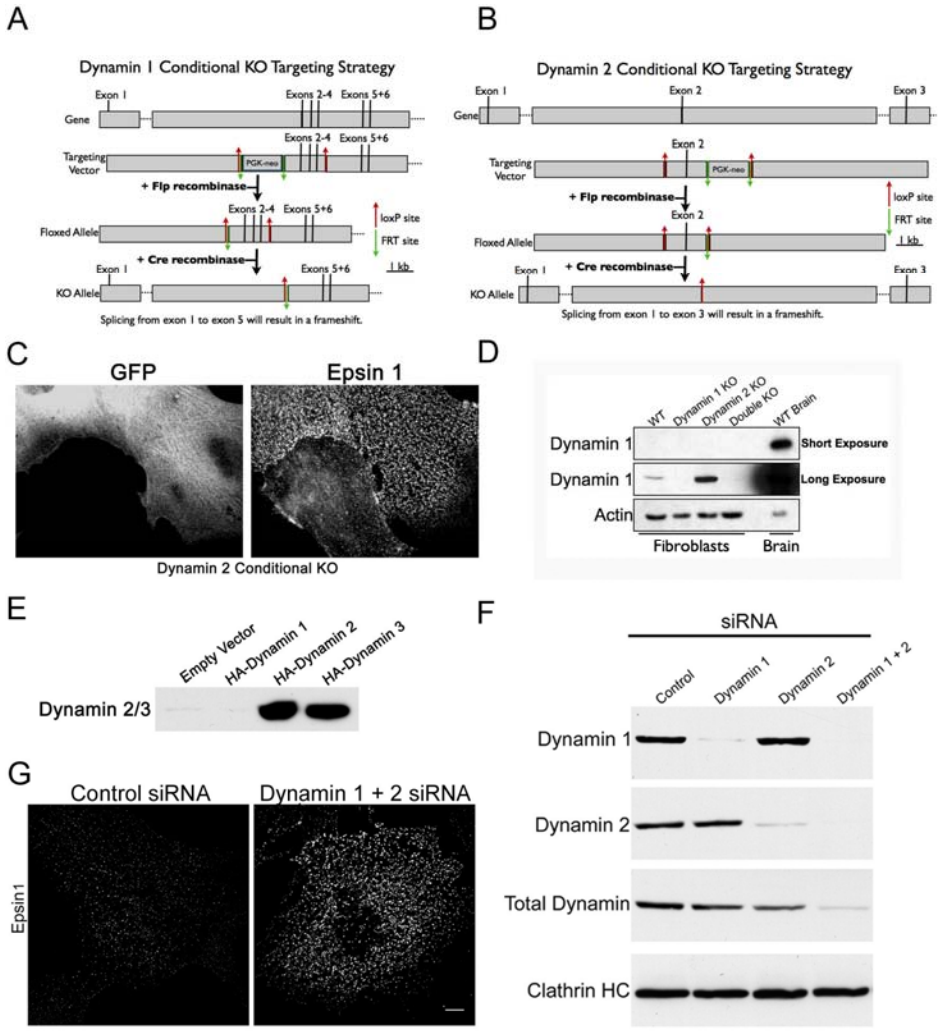

Figure S1

Figure S1. Generation and characterization of DKO cells (related to Figure 1)
(A) Dynamin 1 and (B) dynamin 2 conditional KO gene targeting strategies, respectively. (C) CCPs accumulate in dynamin 2 single conditional KO fibroblasts following Cre recombinase transfection. Dynamin $2^{flox/flox}$ fibroblasts were transfected with a Cre-IRES-GFP bicistronic plasmid and fixed 6 days later. Cells were immunolabeled for GFP and epsin 1 (a CCP protein). Note that the upper cell which expresses the GFP reporter exhibits enhanced CCP staining compared to its untransfected neighbor. However, this phenotype was transient and this was associated with dynamin 1 expression in these cultured fibroblasts.

(D) Dynamin 1 expression in fibroblasts. These immunoblots show that dynamin 1 levels in cultured wildtype fibroblasts are low compared to brain tissue. However, dynamin 1 levels increased in an immortalized line of dynamin 2 KO fibroblasts.
(E) Characterization of a dynamin 2/3 specific antibody (sold as goat anti-dynamin 2 (C-18) by Santa Cruz Biotechnology). Immunoblotting of extracts from COS-7 cells transfected with an empty vector versus HA-tagged mouse dynamin 1, 2 and 3 respectively. This antibody detects the exogenous dynamin 2 and 3 but not dynamin 1. The faint band in the Empty Vector lane corresponds to the endogenously expressed dynamin isoforms of these cells. See also (Ferguson et al, 2007) for further validation of this protocol.
(F) Immunoblotting reveals effective reduction of dynamin 1 and 2 protein levels 3 days after transfection of the indicated siRNAs.
(G) Knockdown of dynamin 1 and 2 results in an accumulation of plasma membrane clathrin-coated pits as assessed by epsin 1 immunofluorescnce.

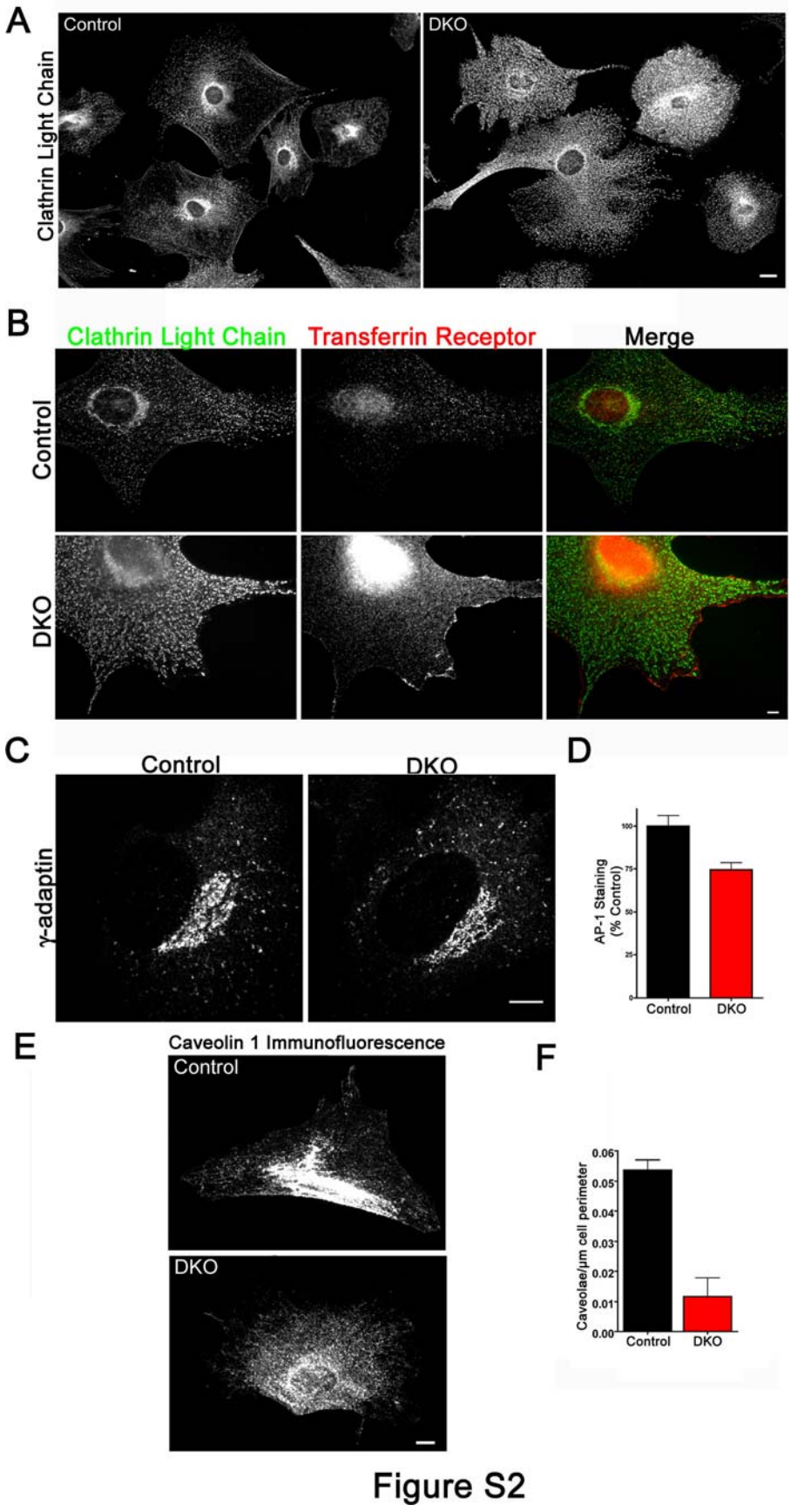

Figure S2

Figure S2. CCP budding from the TGN does not show a defect that parallels the increase in CCP and cargo abundance at the plasma membrane (related to Figure 1)

(A) In control fibroblasts (left panel) CCPs at both the plasma membrane and the Golgi complex are prominent after clathrin light chain immunostaining. In DKO cells (right panel) there is a selective accumulation of CCPs at the plasma membrane.
(B) In addition to an increase in the abundance of plasma membrane CCPs, the DKO cell also exhibits an increase in the plasma membrane localization of endogenous transferrin receptor.
(C) Staining with anti-γ-adaptin (AP-1 component) allowed for a direct investigation of CCPs budding from the TGN. Unlike the what was observed for clathrin coated pits budding from the plasma membrane (see above and Figure 1) the there was no increase in AP-1 staining at the TGN in DKO cells.
(D) Quantification of the γ-adaptin signal within the TGN region (n= 34 and 27 control and DKO cells respectively) supports this conclusion.
(E) Altered localization of caveolin 1 in DKO cells.
(F) Quantification of caveolae abundance at the plasma membrane by electron microscopy. Data was obtained from 3 independent experiments. > 10 cell profiles per genotype were randomly selected for analysis in each experiment ($p=0.0038$, t test). Clathrin light chain, transferrin receptor and caveolin images were captured by epifluorescence microscopy while γ-adaptin was detected by spinning disk confocal microscopy. All results represent immunofluorescent labeling of endogenous proteins. Scale bars = 10μm.

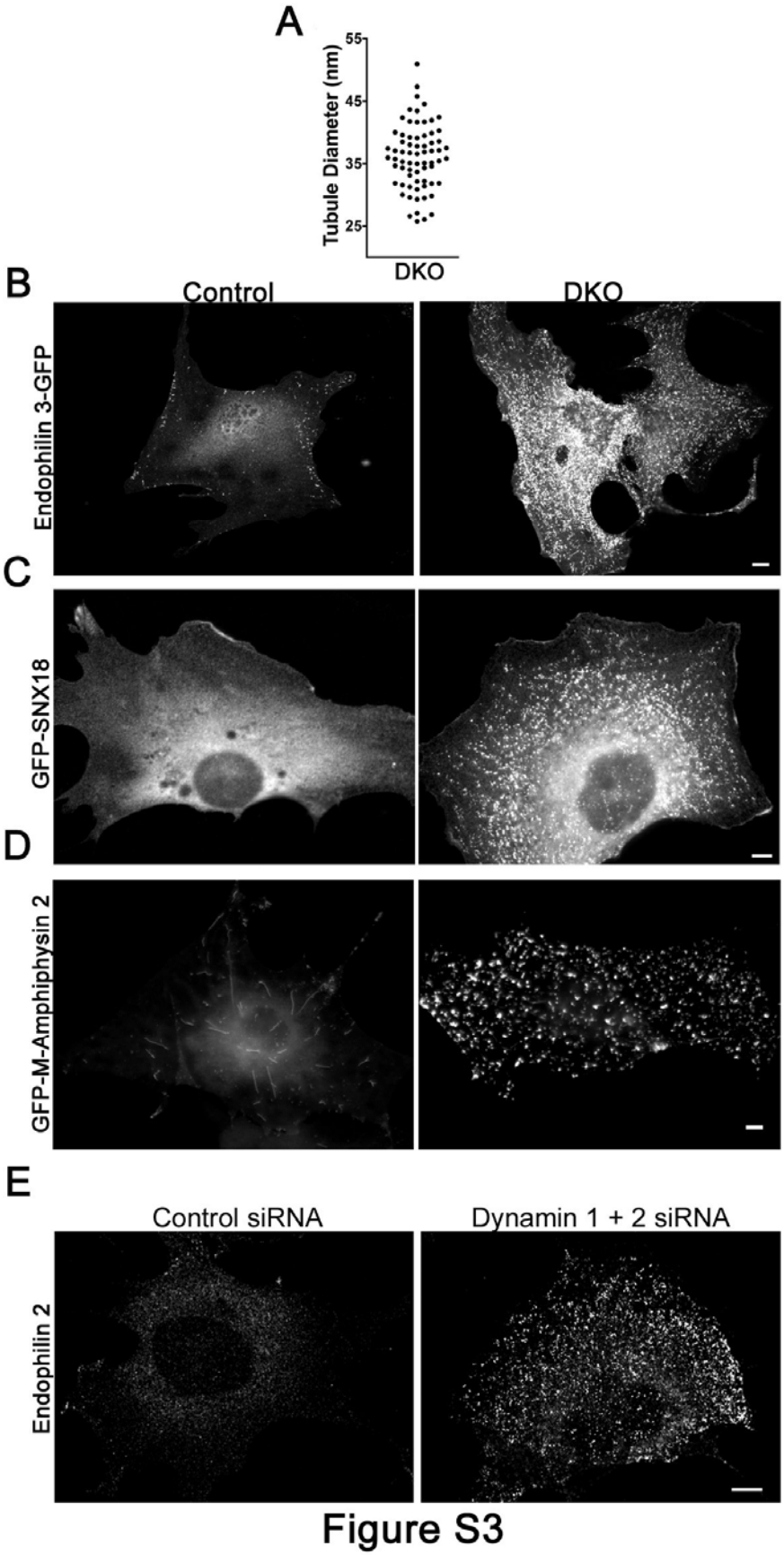

Figure S3

Figure S3. Tubulation at the base of clathrin coated pits in DKO cells is accompanied by the punctate accumulation of dynamin-binding BAR domain proteins (related to Figure 3)

(A) Measurements of tubule cross-section diameter in electron micrographs of DKO cells. Representative examples of such tubule cross-section are indicated by arrows in Figure 2 E, F and G.
(B) Representative localization of Endophilin 3-GFP in control and DKO fibroblasts, respectively.
(C) GFP-SNX18 is also much more punctate in its localization in DKO compared to control cells.
(D) While GFP-M-Amphiphysin 2 forms distinct tubules in control cells, its localization becomes much more clustered in the absence of dynamin.
(E) The endophilin 2 localization is more punctate following siRNA mediated knockdown of dynamin 1 and 2. Images in B-D were obtained by epifluorescence microscopy while spinning disk confocal microscopy was used in (E). Scale bars = 10 μm.

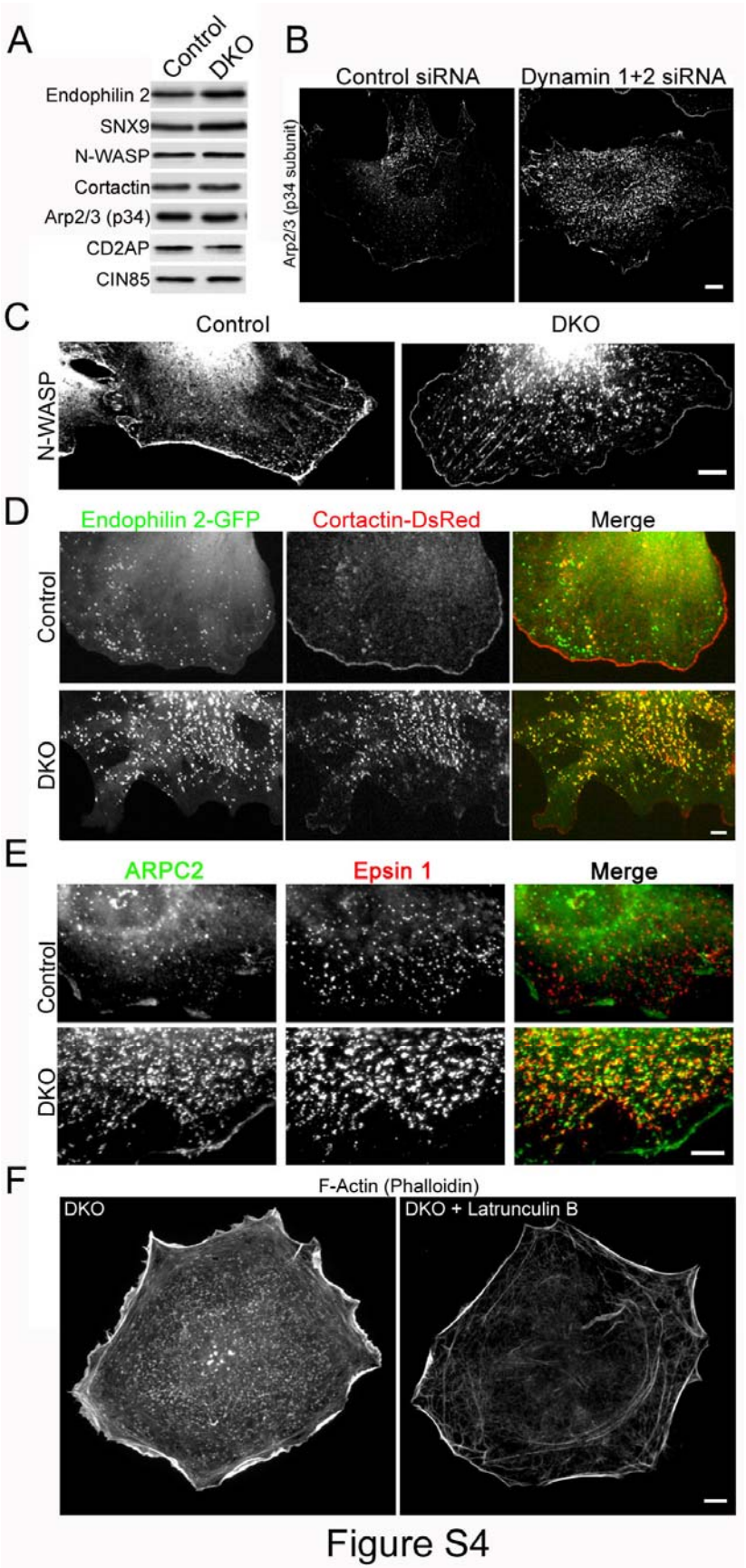

Figure S4. Analysis of expression and localization of dynamin-binding and actin regulatory proteins (related to Figure 4)

(A) Immunoblot comparison of the levels of the indicated proteins in control versus DKO cells. These results confirm the expression of such proteins in our fibroblast cultures.

(B) The localization of the Arp2/3 complex is more punctate following siRNA mediated depletion of dynamin 1 and 2 (spinning disk confocal images of immunofluorescent staining).
(C) Representative immunofluorescence staining of endogenous N-WASP shows a more clustered pattern in the DKO cell.
(D) Endophilin 2-GFP and cortactin-DsRed both accumulate and colocalize in foci at the plasma membrane in DKO cells.
(E) Comparison of Arp2/3 (p34 subunit) and epsin 1 immunofluorescent staining in control and DKO cells respectively. Both proteins exhibit increased staining in the DKO cell and such staining largely overlaps.
(F) The abundant F-actin foci of DKO cells are dispersed within 90 seconds after treatment with 5 μM latrunculin B (phalloidin staining of fixed cells).
Results in C, D-F were obtained by epifluorescence imaging on either live (D) or fixed cells (C, E and F). Scale bars = 10.

Supplemental Experimental Procedures

This section provides a more detailed version of the methods outlined within the main text.

Gene Targeting Strategies

The dynamin 2 (Dnm2 gene symbol, mouse chromosome 9) conditional KO targeting vector was custom made via Red/ET-driven recombineering (GeneBridges, Dresden, Germany). This strategy (Fig. S1) flanked a 1.5kb region containing exon 2 with loxP sites and inserted an FRT site flanked neomycin resistance cassette into intron 2. The targeting vector was electroporated into hybrid C57BL/6J-129S1/Sv mouse embryonic stem cells (Yale Cancer Center Animal Genomics Shared Resource). Following positive-selection, Southern blotting was performed (Gene Dynamics, Portland, OR) to screen colonies for homologous recombination. The identity of positive colonies was verified with both 5' and 3' external probes. Following karyotyping and blastocyst injection, chimeric male offspring were mated to a FLPe recombinase expressing deleter strain (Rodriguez et al., 2000) to remove the neomycin selection cassette. The absence of the neomycin selection cassette in the FLPe-positive offspring from these matings was confirmed by PCR and these mice were used in subsequent dynamin 2 conditional KO studies. Animal care and use was carried out in accordance with our institutional guidelines.
The dynamin 1 (Dnm1 gene symbol, mouse chromosome 2) conditional KO targeting vector (Vector BioLabs, Philadelphia, PA) flanked exons 2-4 with loxP sites, inserted an FRT site flanked neomycin resistance selection cassette into intron 1 and contained a 5' thymidine kinase negative selection cassette (Fig. S1). Subsequent gene targeting and screening was performed as described above.
Conditional mutants were crossed with two different Cre deleter strains: (i) a beta actin-Cre mouse (FVB/N-Tg(ACTB-cre)2Mrt/J) (Lewandoski et al., 1997) was used to inactivate the Dnm2 gene ubiquitously (including in the germline), so that a constitutive Dnm2 KO allele could be generated; (ii) a tamoxifen-inducible Cre strain (B6;129-Gt(ROSA)26Sor$^{tm1(cre/Esr1)Nat}$/J) (Badea et al., 2003) (Jackson Lab, Bar Harbor, ME) was crossed with Dnm1$^{LoxP/LoxP}$ /Dnm2$^{LoxP/LoxP}$ mice to generate mutants in which Dnm1/2 gene ablation could be induced in a temporally-controlled fashion. Genotyping of recombinant mice was either performed in house by PCR analysis or by Transnetyx (Cordova, TN).

Fibroblast Cultures

Fibroblasts were isolated from mice from the age of embryonic day 12 to post-natal day 1 by the 3T3 method (Todaro and Green, 1963). Cells were grown in DMEM (containing glutamine) + 10% fetal bovine serum + 1% penicillin/streptomycin supplement. Cell culture reagents were purchased from Invitrogen (Carlsbad, CA). Cre adenovirus was purchased from the University of Iowa Gene Transfer Vector Core (Iowa City, IA). Cre retrovirus was prepared by the transfection

of Phoenix-Eco packaging cells (ATCC, Manassas, VA) with a Cre recombinase encoding pBABE-puro plasmid. Supernatant from such cells was harvested, filtered and following addition of 8µg/ml polybrene (Sigma, St Louis, MO) was used to transduce fibroblasts. 24 hours later Cre recombinase positive cells were selected with 2.5µg/ml puromycin (Sigma). For the tamoxifen-inducible KO, cells were treated with 2 sequential 24 hour incubations with 3µM 4-hydroxy-tamoxifen (Sigma). Regardless of the method used to achieve the conditional KO, maximal dynamin 1+2 depletion was achieved within 5 days. Cells were generally used for experiments between 6 and 9 days after Cre recombinase delivery/activation. Examination of DKO cells at up to 3 weeks after Cre delivery/activation did not reveal the emergence additional phenotypes leading us to conclude that the phenotype achieved by 6 days is both maximal and stable. Due to the proliferation defect of the DKO cells, overgrowth of the cultures by cells that avoided dynamin recombination was frequently a problem at longer time points (beyond 10 days). While such challenges could be at least partially overcome in the tamoxifen-inducible Cre line by maintaining a low concentration (100-300nm) of 4-hydroxy-tamoxifen in the culture medium, it was in general most practical to use the DKO cells within the 6-9 day post-tamoxifen interval. In the described experiments, both early passage primary fibroblast cultures and immortalized (3T3 method) fibroblasts gave equivalent results.

Antibodies

Immunoblotting of cultured fibroblasts was performed by previously described methods (Ferguson et al., 2007). Antibodies for immunoblotting and immunofluorescence were obtained from the following commercial sources: rabbit anti-dynamin 1 (Epitomics, Burlingame, CA), goat anti-dynamin 2/3 (Santa Cruz Biotechnology, Santa Cruz, CA), rabbit anti-caveolin (BD Biosciences, San Jose, CA), mouse anti-tubulin and mouse anti-acetylated-tubulin (Sigma), mouse anti-transferrin receptor antibody and rabbit anti-GFP (Invitrogen), rabbit anti-ARPC2 and mouse anti-cortactin (Millipore, Billerica, MA). The following antibodies were kind gifts: rabbit anti-N-WASP (Marc Kirschner, Harvard University Boston, MA), rabbit anti-SNX9 (Sven Carlsson, Umea University, Sweden), rabbit anti-CD2AP and CIN85 (Andrey Shaw, Washington University, St. Louis, MO) and mouse anti-epsin 1 (Pier-Paolo Di Fiore, IFOM, Milan, Italy). Other antibodies were previously described (Ringstad et al., 1997; Itoh et al., 2005; Ferguson et al., 2007); Hayashi et al., 2008). Alexa594-phalloidin as well as Alexa488 and alexa594-conjugated secondary antibodies were from Invitrogen.

siRNA Transfection

3 days after starting OHT or vehicle treatment, cells (150,000/transfection) were transfected with siRNA (150 pmol/transfection, IDT) using RNAiMAX (5µl/transfection, Invitrogen) and were used for experiments 3-5 days later to allow for combined dynamin 1, dynamin 2 and clathrin heavy chain or Arp2/3 p34 degradation. siRNA sequences were as follows: Control 5'-CUUCCUCUCUUUCUCUCCCUUGGA-3' annealed to 5'-UCACAAGGGAGAGAAAGAGAGGAAGGA-3' and CHC 5'-GGAAAGUUACAUAUCAUUGAAGUTG-3' annealed to 5'-CAACUUCAAUGAUAUGUAACUUUCCUC-3'. Comparable results were observed with three additional CHC siRNA sequences. The p34 siRNA consisted of: 5'-GGAGUUCAAAGAAGGACGCAGAGCC-3' annealed to 5'-GGCUCUGCGUCCUUCUUUGAACUCCUG-3'. Dynamin 1 and 2 siRNA experiments were performed in control fibroblasts and cells were analyzed 3-4 days after transfection. The dynamin 1 siRNA duplex consisted of: 5'-GGCUUACAUGAAUACCAACCACGAA-3' annealed to 5'-UUCGUGGUUGGUAUUCAUGUAAGCCAG-3' and the dynamin 2 siRNA duplex was: 5'-GAAUGAGGAUGGAGCACAAGAGAAC-3' annealed to 5'-GUUCUCUUGUGCUCCAUCCUCAUUCUC-3'.

Cell Proliferation Assays

For cell counting, control and DKO fibroblasts were plated at 50000 cells per 35 mm dish. Three dishes of cells were subsequently counted in duplicate using a hemacytometer both 1 and 3 days later and the ratio of the cell numbers from these two days was taken as an index of proliferation. For bromodeoxyuridine (BrDU) labeling, Control and DKO fibroblasts were plated at 10,000 cells per 12mm coverslip. Cells were incubated for 6 hours with 10 μM BrDU (Invitrogen), fixed with Carnoy's fixative (3 parts methanol:1 part glacial acetic acid) at -20^{o}C for 20 minutes, 2M HCl treated at room temperature for 20 minutes to denature DNA, labeled with Alex594 conjugated anti-BrDU antibody (Invitrogen) and co-stained with DAPI.

Transferrin Uptake and Transferrin Receptor Localization

For transferrin uptake, cells were electroporated (Nucleofector, Amaxa, Cologne, Germany) with a plasmid encoding GFP (pHluorin)-tagged human transferrin receptor (Merrifield et al., 2005). Such expression of human transferrin receptor overcame limitations arising from the low abundance of the endogenous transferrin receptor and its relatively low affinity for the fluorescently labeled human transferrin used in our uptake assays. One day after electroporation, cells were rinsed with serum-free DMEM and incubated for 15 minutes with 10μg/ml Alexa594 conjugated human transferrin (Invitrogen) to allow for transferrin uptake. The assay was ended by rinsing the cells with ice cold PBS and fixing with 4% paraformaldehyde-0.1M sodium phosphate pH 7.2. Transferrin receptor-GFP was localized by staining with rabbit anti-GFP primary antibody (Invitrogen) and Alexa488 conjugated goat anti-rabbit secondary antibody (Invitrogen). Similar localization results were obtained upon staining of the endogenous transferrin receptor (Fig. S2).

Transferrin Receptor Biotinylation

Cell were rinsed with PBS, and labeled on ice for 60 minutes with 1mg/ml EZ-link Sulfo-NHS-SS-Biotin (Thermo Scientific, Rockford, IL), rinsed with Tris buffered saline (TBS) and lysed in TBS containing 1% TX100 and 0.1%SDS and protease inhibitor cocktail (Roche, Indianapolis, IN). Biotinylated proteins were recovered on neutravidin beads (Thermo Scientific) and eluted by reduction with 2-mercaptoethanol containing SDS-PAGE sample buffer. Evaluation of transferrin receptor levels in starting material, biotinylated (cell surface) and non-biotinylated (intracellular) fractions was assessed by immunoblotting following SDS-PAGE. Actin immunoblotting (mouse anti-actin antibody, Sigma) was used as a negative control to ensure that the assay specifically distinguished between cell surface and intracellular proteins.

FM1-43FX Uptake

Control and DKO fibroblasts were plated at 10,000 per 12mm coverslips, incubated for 30 minutes at 37^{o}C in 5μg/mL FM1-43FX (fixable analog of FM1-43, Invitrogen) in the following buffer: 136mM NaCl, 2.5mM KCl, 2mM CaCl2, 1.3mM MgCl, 10mM HEPES. Cells were washed 4 x 5minutes, and fixed in 4% paraformaldehyde-0.1M sodium phosphate pH 7.2. Coverslips were finally mounted in Prolong Gold (Invitrogen) and were imaged as for the immunofluorescence experiments described below.

Electroporation, plasmids and reagents

Cells for imaging experiments were electoporated with the Amaxa Nucleofector method and were plated at sub-confluent densities into 2.5μg/ml human fibronectin (Millipore)-coated 35 mm glass bottom (thickness=1.5) dishes (Mattek, Ashland, MA) and allowed to grow for 12 to 48 hours prior to imaging. Clathrin light chain-GFP was a gift from James Keen (Thomas Jefferson University, Philadelphia, PA), dynamin 2-GFP and dynamin 2-ΔPRD-GFP were generously provided by Mark McNiven (Mayo Clinic, Rochester, MN), clathrin light chain-mRFP, GFP-amphiphysin 2 and endophilin 2-GFP plasmids were previously described (Lee et al., 2002; Perera et al., 2006). Cortactin-DsRed, Myo1e-GFP and CD2AP-GFP were kindly

provided by David Zenisek (Yale University), Mark Mooseker (Yale University) and Andrey Shaw (Washington University, St. Lousi) respectively. In some experiments, endophilin 2-GFP (pBABE-puro plasmid) was delivered via a retroviral transduction following packaging in Phoenix-Eco cells (ATCC, Manassas, VA). For the GFP-tagged N-WASP construct, the N-WASP coding sequence was PCR amplified from mouse brain cDNA (BD Clontech) and ligated into the pEGFP-C3 plasmid (BD Clontech) to generate an in frame N-terminal GFP fusion. The GFP-SNX9 was a N-terminal fusion in the pcDNA3 plasmid and was kindly provided by Kai Erdmann. Mouse SNX18 was amplified from clone BC063089.1 (Open Biosystems, Huntsville, AL) by PCR and ligated into pEGFP-C1 to make an N-terminal fusion. CD2AP-GFP was kindly provided (Washington University, St. Louis, MO). Latrunculin B was purchased from Calbiochem, (San Diego, CA), dissolved in DMSO and used at a final concentration of 5μM.

Immunofluorescence

Cells were grown on either untreated or 5μg/ml fibronectin (Millipore) coated glass coverslips and were fixed with 4% paraformaldehyde-0.1M sodium phosphate pH 7.2. Coverslips were washed with 50mM NH_4Cl pH 7.2 then blocked and permeablized with PBS+3% bovine serum albumin + 0.1% TX100. Subsequent primary and secondary antibody incubations were made in this buffer. Coverslips were finally mounted in Prolong Gold (Invitrogen). For epifluorescence imaging, samples were imaged with a Zeiss Axioplan2 microscope using a Plan-Apochromatic 40x objective and a Hamamatsu (Bridgewater, NJ) ORCA II digital camera under the control of MetaMorph v7.1.2 software (Molecular Devices, Sunnyvale, CA). Alternatively, as indicated immunofluorescence data was also acquired b y spinning disk confocal microscopy (see below).

For rescue experiments, cell were electroporated with the indicated plasmids, fixed 18 hours later and immunostained for the indicated protein Images were acquired from the bottom surface of the cell by spinning disk confocal microscopy and the abundance of α-adaptin, endophilin 2 and Arp2/3 (p34) were quantified using either Volocity or ImageJ software. Adjustments to contrast and thresholding were made in a uniform manner to all images within a dataset, spots were detected and the spot number or area occupied by spots (i.e. clathrin-coated pits) was normalized to the total area of the cell.

Widefield Video Microscopy

Imaging was performed at 30-37°C in the following buffer: 136mM NaCl, 2.5mM KCl, 2mM CaCl2, 1.3mM MgCl, 10mM glucose, 10mM HEPES supplemented with 2.5% fetal bovine serum. Time-lapse widefield epi-fluorescent images were acquired with a Leica AM6000 inverted microscope equipped with Plan- Apochromatic 40X oil and 63X glycerol immersion objectives, and a CoolSnap HQ CCD camera (Photometrics, Pleasanton, CA). A 470/30 nm excitation and 520/35 emission filter was used for GFP imaging. Image capture and data acquisition were performed using Metamorph software V7.0r1. Images were acquired at 0.25-0.5 Hz and exposure times of 100-300 ms. Images sequences were subsequently processed with Metamorph and ImageJ software (1.40g, NIH).

Spinning Disk Confocal Microscopy

Spinning disc confocal microscopy was performed using the Improvision (Waltham, MA) UltraVIEW VoX system including a Nikon Ti-E Eclipse inverted microscope (equipped with 60x CFI PlanApo VC, NA 1.4, and 100x CFI PlanApo VC, NA 1.4 objectives) and a spinning disk confocal scan head (CSU-X1, Yokogawa) driven by Volocity (Improvision) software. Images were acquired without binning with a 14 bit (1000x1000) Hamamatsu (Bridgewater, NJ) EMCCD. Illumination was provided by Coherent solid state 488 nm/50 mW diode and Cobolt (Stockholm, Sweden) solid state 561 nm/50 mW diode lasers. Emission filters for GFP and RFP were: a 527 nm band single band pass center wavelength (CWL), 55 nm half-power bandwidth (FWHM) and a double band pass 500-548 nm and 582-700 nm respectively. Typical exposure

times and acquisition rates were 100-300 ms and 0.25 Hz respectively. Cells were imaged at temperatures ranging from 23-37°C. Where indicated, images were taken at 100 nm intervals in the Z-axis, iteratively deconvolved with Volocity software and presented as maximal projections. Background signals were reduced by the use of a 3 pixel filter (Volocity). Post-acquisition image analysis was performed with Volocity as well as ImageJ software.

Electron Microscopy

Control and DKO fibroblasts (~80% confluent) in 60mm dishes were fixed in 2% glutaraldehyde-0.1M sodium cacodylate. After gentle scraping and pelleting, subsequent electron microscopy and tomography procedures were performed as previously described (Ferguson et al., 2007; Hayashi et al., 2008). For morphometric analysis, cells were selected at a low magnification that allowed confirmation that the entire outer perimeter was intact but at which clathrin-coated pits themselves were not visible so as to make the selection process blind with respect to the phenotype of interest. Once selected, higher magnification images were taken around the periphery of the cell and clathrin-coated structures within the categories defined in Fig. 2H that were within 500 nm of the plasma membrane were counted all the way around the perimeter of each cell. For cells undergoing latrunculin B treatment prior to fixation, the cells were rinsed 3 times with 136mM NaCl, 2.5mM KCl, 2mM CaCl2, 1.3mM MgCl, 10mM glucose, 10mM HEPES, incubated for 10 minutes at 37°C in this buffer, incubated 90 seconds more in the presence of 5µM latrunculin B then fixed with 2% glutaraldehyde-0.1M sodium cacodylate. Phalloidin staining of paraformaldehyde fixed samples confirmed that this treatment abolished the highly punctate F-actin staining of the DKO cells while only partially disassembling stress fibers (Fig. S4).

SUPPLEMENTAL REFERENCES

Badea, T.C., Wang, Y., and Nathans, J. (2003). A noninvasive genetic/pharmacologic strategy for visualizing cell morphology and clonal relationships in the mouse. J Neurosci 23, 2314-2322.

Ferguson, S.M., Brasnjo, G., Hayashi, M., Wolfel, M., Collesi, C., Giovedi, S., Raimondi, A., Gong, L.W., Ariel, P., Paradise, S., et al. (2007). A selective activity-dependent requirement for dynamin 1 in synaptic vesicle endocytosis. Science 316, 570-574.

Itoh, T., Erdmann, K.S., Roux, A., Habermann, B., Werner, H., and De Camilli, P. (2005). Dynamin and the actin cytoskeleton cooperatively regulate plasma membrane invagination by BAR and F-BAR proteins. Dev Cell 9, 791-804.

Lee, E., Marcucci, M., Daniell, L., Pypaert, M., Weisz, O. A., Ochoa, G. C., Farsad, K., Wenk, M.R., and De Camilli, P. (2002). Amphiphysin 2 (Bin1) and T-tubule biogenesis in muscle. Science 297, 1193-1196.

Lewandoski, M., Meyers, E.N., and Martin, G.R. (1997). Analysis of Fgf8 gene function in vertebrate development. Cold Spring Harb Symp Quant Biol 62, 159-168.

Merrifield, C.J., Perrais, D., and Zenisek, D. (2005). Coupling between clathrin-coated-pit invagination, cortactin recruitment, and membrane scission observed in live cells. Cell 121, 593-606.

Perera, R.M., Zoncu, R., Lucast, L., De Camilli, P., and Toomre, D. (2006). Two synaptojanin 1 isoforms are recruited to clathrin-coated pits at different stages. Proc Natl Acad Sci U S A 103, 19332-19337.

Ringstad, N., Nemoto, Y., and De Camilli, P. (1997). The SH3p4/Sh3p8/SH3p13 protein family: binding partners for synaptojanin and dynamin via a Grb2-like Src homology 3 domain. Proc Natl Acad Sci U S A 94, 8569-8574.

Rodriguez, C.I., Buchholz, F., Galloway, J., Sequerra, R., Kasper, J., Ayala, R., Stewart, A. F., and Dymecki, S. M. (2000). High-efficiency deleter mice show that FLPe is an alternative to Cre-loxP. Nat Genet 25, 139-140.

Todaro, G.J., and Green, H. (1963). Quantitative studies of the growth of mouse embryo cells in culture and their development into established lines. J Cell Biol 17, 299-313.